Performance Model for Orthogonal Sub Channel in Noise-limited Environment

Jyrki T.J. Penttinen, Francesco D. Calabrese
Nokia Siemens Networks Innovation Center (NICE)
Madrid, Spain
jyrki.penttinen@nsn.com
francesco.calabrese@nsn.com

David Valerdi, Iñigo Güemes
Vodafone Center of Competence (CoC)
Madrid, Spain
david.valerdi1@vodafone.com
inigo.guemes@vodafone.com

***Abstract*—OSC (Orthogonal Sub Channel) is an enhancement for the GSM voice service. It provides up to double capacity in the radio interface with the same hardware compared to the GSM Half Rate (HR) mode. This paper investigates the effects of OSC on the capacity utilization as a function of the OSC capable handset penetration. The variation of the radio network capacity is studied by taking into account the division of the time slot usage between HR and OSC capable terminals, which depends on the OSC capable handset penetration. The achievable capacity gain is studied by investigating the blocking rate behavior. In addition, a set of test cases was carried out in a GSM network in order to evaluate the radio performance of OSC in terms of the carrier per noise level. The tests were performed in a noise-limited indoor environment, and the quality and received power level distributions were analyzed. Based on the post-processing and analysis of the performance data as a function of the OSC penetration, a generic model to estimate the effect of OSC on the GSM capacity gain was developed. The model utilizes the network statistics and performance indicators of GSM, and provides an estimate of the possible OSC gains in the investigated regions before the OSC feature is actually activated.**

***Keywords*—OSC, GSM, 2G, SAIC, voice evolution, capacity enhancement, radio network planning, optimization, DHR.**

I. INTRODUCTION

The capacity utilization is one of the most important optimization items of the GSM radio interface. The recently developed Dual Half Rate (DHR) functionality can be considered as a major step in the 2G evolution path. OSC (Orthogonal Sub Channel) is a solution for offering the pairing of two separate users into a single HR (Half Rate) time slot resource in such a way that no hardware enhancements are needed in the network side. OSC utilizes a SAIC (Single Antenna Interference Cancellation) functionality of the already existing handsets, which means that OSC provides a SAIC penetration dependent capacity gain as soon as it is activated via a software update of the Base Transceiver Stations (BTS) and Base Station Controllers (BSC) of the GSM radio network.

Based on [1], this paper presents an extended analysis of the OSC gain as a function of SAIC handset penetration, and complements the analysis by investigating further the radio performance analysis presented in [2]. These results are processed in order to form a complete OSC gain model that consists of the predicted effect on the capacity and radio performance of GSM voice calls.

During the evolution of the circuit switched (CS) domain of GSM, there have been various capacity enhancement methods applied in the networks like Dynamic Frequency and Channel Allocation [3], Adaptive Multi Rate codecs [4] and Frequency Hopping (FH) [5]. Also several other solutions have been proposed, although these are still under development, like multiple beam smart antennas [6]. At the moment, though, one of the most concrete ways that provide with a notable capacity effect is the SAIC concept. There are various studies available presenting the respective benefit in different environments [7][8][9][10].

The first DHR deployments are based on the OSC functionality that has been evaluated and standardized by 3GPP GERAN [11][12][13][14]. It utilizes SAIC and provide capacity enhancement without need for modifications to the already existing new mobile station generation.

Despite of the availability of various studies about the SAIC gain, the capacity behavior in a typical OSC network deployment is not clear. This paper presents thus an analysis of the effect of OSC on the offered capacity by investigating the benefits, e.g., in terms of the utilization and possibility for the reduction of the transceivers as a part of the frequency re-farming between GSM and other technologies such as HSPA (High Speed Packet Access) and LTE (Long Term Evolution). Based on realistic radio measurements in an indoor environment, this paper also investigates the effective proportion of the coverage area where OSC can be utilized.

The GSM HR mode is selected as a reference for the investigations as it is assumed to be available in a typical environment. The capacity gain of OSC is obviously lower in the cell edge where the network dependent algorithm switches the OSC first to the HR mode and eventually to the FR (Full Rate) mode assuming that Adaptive Multi Rate (AMR) functionality is utilized. This paper investigates the capacity effect of OSC together with the impacts on the radio quality, which together forms a complete prediction model for the OSC gain as a function of the OSC penetration.

First, a brief overview to the principles and functionality of OSC is given in Section II. Then, a theoretical analysis of

the capacity behavior of OSC is presented in Section III. The analysis shows the mapping of the estimated OSC penetration value in the actual usage of the Time Slots (TSL) for OSC and GSM Half-Rate (HR) modes. Then, the effect of OSC is investigated on the variation of the offered traffic, which gives possibility to estimate either the reduction of the already deployed capacity (transceiver units, TRX) or, which gives time for the postponing of the future hardware capacity additions yet maintaining the original or lower blocking rate of the GSM cell. The effects of OSC on the radio performance are investigated in Section IV, which provides information about the usability of OSC within the coverage area. The field tests carried out in this section are based on the noise-limited indoor environment, but the results can be extended also to the outdoor. Based on Sections III and IV, the complete model is proposed in Section V. The input of the model is based on the Key Performance Indicators (KPI) of GSM. The output predicts the effect of OSC on the respective OSC coverage compared to the GSM HR (Half Rate) mode as a function of the OSC penetration. Finally, Section VI presents the conclusions of the work.

II. THE FUNCTIONALITY AND USABILITY OF OSC

GSM technology is globally most widely deployed cellular mobile communication system. In emerging markets, the increase trend of new-developed subscribers and consequent voice traffic explosion creates a great pressure on network operators, especially for those operators that need to provide service to a large population with only limited bandwidth. In mature markets, GSM frequencies are being re-farmed to UMTS and LTE in order to provide a national-wide mobile broadband service with a limited investment and better quality; this action will squeeze GSM bandwidth and increase demand over GSM technology to achieve higher capacity and spectrum efficiency, so as to maintain the current traffic volumes and user experience. Furthermore, considering that the Average Revenue per User (ARPU) continues decreasing, most operators are facing the challenge of improving their hardware utilization efficiency.

In order to cope with the scenarios outlined above, some possible solutions are brought up. Among them, one of the most promising proposals is the OSC feature, a voice capacity enhancement for the GSM networks. OSC is standardized in 3GPP, and the first live network OSC trials have been carried out in 2010. OSC is backwards compatible solution with the original TDMA frame structure of GSM, exploiting the single 200 kHz frame bandwidth by multiplexing more users to its 8 physical time slots. The OSC DHR (Dual Half Rate) mode utilizes a single physical TSL for up to four users compared to the HR mode that can multiplex two users within the same TSL, or only one user in the FR (Full Rate) mode.

In Downlink (DL), OSC DHR distinguishes between two independent GSM users sharing the same HR resource by interpreting the 8-level GMSK modulation as two separate QPSK (Quadrature Phase Shift Keying) modulation diagrams in such a way that the users form pairs within the HR TSL as presented in FIGURE 1.

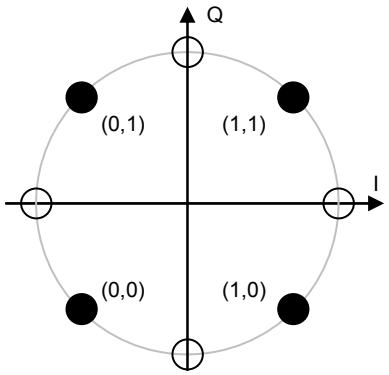

FIGURE 1. Two separate OSC DHR users can be multiplexed in DL via the pairing based on the QPSK constellation.

As presented in FIGURE 2, a MUD (Multi-User Detection) receiver is used in Uplink (UL) in order to identify two users sharing the same physical time slot, and the separation of the users is handled via different training sequences [11]. This requires antenna diversity in the GSM base station with MUD functionality [9]. The applied Multiple-Input, Multiple-Output (MIMO) concept gives benefits especially in Rayleigh fading channel [12]. A GMSK modulation is used in UL.

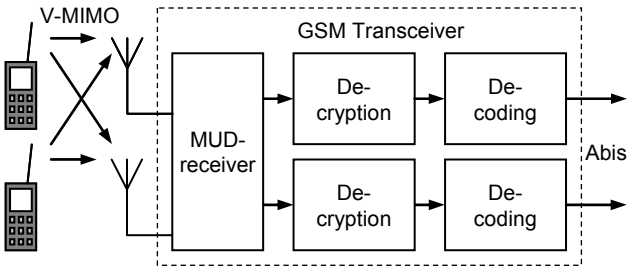

FIGURE 2. Two OSC DHR users can share the same HR resource in UL via the MIMO functionality of MUD.

FIGURE 3 shows an example about the average behavior of the OSC DHR and HR calls in a fully occupied 8-TSL TRX assuming that the OSC penetration is 50% and that the users are uniformly distributed over the investigated area.

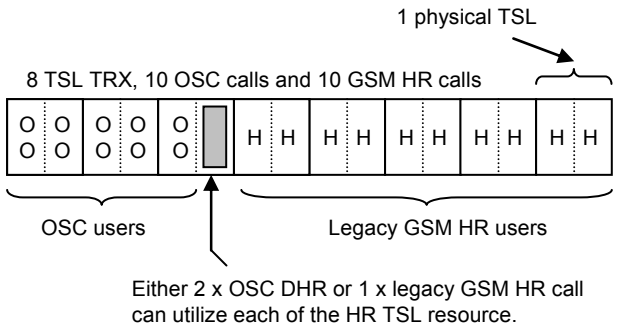

FIGURE 3. An example of the utilization of the TRX resources for OSC DHR and GSM HR calls with the same OSC (SAIC) terminal penetration.

As FIGURE 3 indicates, the TSL division for the OSC and HR calls can be estimated to be 1:2 in case of 50% OSC penetration, i.e., OSC utilizes 1/3 of the physical TSL resources in this case.

When the radio conditions are ideal, i.e., there are no restrictions from the radio network side in the usage of the TSL for OSC DHR, HR or FR calls, it is thus possible to fit 2 times more OSC DHR calls into the same TSL compared to HR calls.

The following analysis shows the more detailed division of the TSL utilization for the OSC DHR and HR users as a function of the OSC penetration, assuming that the network supports both modes in the normal operation.

III. EFFECT OF OSC ON CAPACITY

This analysis shows the behavior of the GSM cell capacity when both GSM HR and OSC DHR users are found in the area. More specifically, the distribution of the HR and OSC users in the same cell is studied as a function of the OSC capable SAIC mobile station penetration. The capacity enhancement is shown between the extreme values, i.e., when only HR users are found, and when the cell is populated with OSC users, in a fully loaded cell.

In the scenarios presented in this paper, it is assumed that the functionality of the OSC is ideal, i.e., it is transparent for the existing HR traffic, and that there is no impact of the feature on the previous functionality of the network. It should be noted that this analysis concentrates purely on the radio interface time slot capacity, and does not consider the effects of the feature on the radio link budget. The assumption of these calculations is thus the presence of a coverage area where the quality and received power levels are sufficiently high for the functioning of the OSC.

The benefit of OSC is obvious in a fully loaded network where major part of the GSM Mobile Stations (MS) is OSC capable. The presented investigations are divided into three scenarios: The effect of OSC DHR on the TSL distribution in a fully loaded cell, on the number of users per TSL, and on the blocking rate, which can result the possibility to reduce TRX units from the GSM sites.

A fully loaded cell can be taken as a basis for the study. The assumption is that both HR and OSC capable users are uniformly distributed over the investigated area. This means that the OSC capable MS penetration equals to the probability of the OSC MS entering to the cell, the rest of the MSs entering to the cell utilizing the HR mode. It should be noted that the term HR refers to a MS that is capable of utilizing both HR and FR modes.

When the OSC feature is activated in the GSM network, the total number of users, i.e., Mobile Stations that are distributed in the investigated area, is a mix of OSC DHR users and GSM HR users:

$$N_{MS}^{tot} = N_{MS}^{OSC} + N_{MS}^{HR} \quad (1)$$

The amount of the OSC users depends on the OSC capable MS penetration α with $\{\alpha \in \mathbb{R} | 0 \leq \alpha \leq 1\}$. The number of OSC capable users is thus:

$$N_{MS}^{OSC} = \alpha \cdot N_{MS}^{tot} \quad (2)$$

This means that the number of HR users is:

$$N_{MS}^{HR} = (1-\alpha) \cdot N_{MS}^{tot} \quad (3)$$

The total number of physical TSLs is divided to the TSLs utilized by the OSC users and the HR users. The expression for the TSLs occupied by the OSC and HR users is thus:

$$N_{TSL}^{tot} = N_{TSL}^{OSC} + N_{TSL}^{HR} \quad (4)$$

The formula contains physical TSLs for OSC and HR. As a single OSC TSL can be utilized by a total of 4 OSC users, we can present the relationship between the TSL and the number of the users in the following way:

$$N_{MS}^{OSC} = 4 \cdot N_{TSL}^{OSC} \quad (5)$$

Equally, a total of 2 HR users can utilize the TSL, which can be expressed as:

$$N_{MS}^{HR} = 2 \cdot N_{TSL}^{HR} \quad (6)$$

FIGURE 4 clarifies the idea of the notation. In this specific case, the OSC user penetration α is 12 / 22 = 55%, and the physical TSL utilization for OSC users is 3/8.

Assuming that the users are distributed uniformly in the coverage area, the utilization of the TSLs depends on the OSC penetration. The following analysis represents the best case scenario of a number of HR MSs, which is multiple of 2 and a number of OSC MSs, which is multiple of 4 so that no TSL is occupied by less than 4 OSC MSs or less that 2 HR MSs.

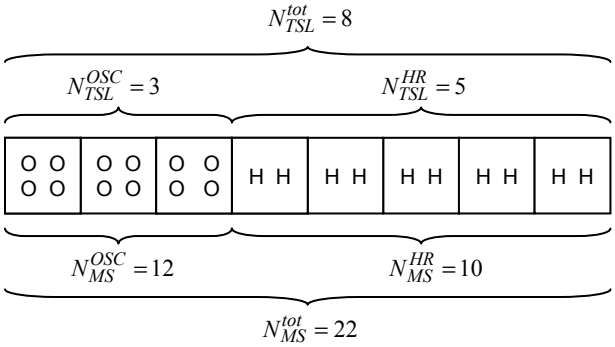

FIGURE 4. An example of the utilization of a single TRX by OSC (marked as O) and HR (marked as H) users.

By combining (4), (5) and (6), we can write:

$$N_{TSL}^{tot} = N_{TSL}^{OSC} + N_{TSL}^{HR} = \frac{N_{MS}^{OSC}}{4} + \frac{N_{MS}^{HR}}{2} \quad (7)$$

We can then introduce the dependency from the OSC penetration using (2) and (3):

$$N_{TSL}^{tot} = \frac{\alpha \cdot N_{MS}^{tot}}{4} + \frac{(1-\alpha) N_{MS}^{tot}}{2} \quad (8)$$

We have therefore expressed the total number of needed TSLs as a function of the total number of MSs and the OSC penetration coefficient.

A. The number of users as a function of α

Similarly, we can express the total number of MSs that can be served as a function of the total number of available TSLs and the OSC penetration coefficient.

Let's then introduce β with $\{\beta \in \mathbb{R} | 0 \le \beta \le 1\}$, which gives the percentage of the physical TSLs occupied for the OSC users. The analysis can be carried further and we can write:

$$\begin{aligned} N_{MS}^{tot} &= N_{MS}^{OSC} + N_{MS}^{HR} \\ &= \beta \cdot N_{TSL}^{tot} \cdot 4 + (1-\beta) \cdot N_{TSL}^{tot} \cdot 2 \\ &= 2 \cdot N_{TSL}^{tot} \cdot (2\beta + 1 - \beta) \\ N_{MS}^{tot} &= 2 \cdot (1+\beta) \cdot N_{TSL}^{tot} \end{aligned} \quad (9)$$

We can rearrange as follows:

$$\begin{aligned} N_{TSL}^{tot} &= \frac{\alpha \cdot N_{MS}^{tot}}{4} + \frac{(1-\alpha) \cdot N_{MS}^{tot}}{2} \\ &= \frac{\alpha \cdot N_{MS}^{tot} + 2 \cdot (1-\alpha) N_{MS}^{tot}}{4} \\ N_{TSL}^{tot} &= \frac{(2-\alpha)}{4} N_{MS}^{tot} \end{aligned} \quad (10)$$

The total number of users can then be expressed as a function of the TSLs:

$$N_{MS}^{tot} = \frac{4 \cdot N_{TSL}^{tot}}{2-\alpha} \quad (11)$$

By comparing (9) and (11) we obtain:

$$\frac{4 \cdot N_{TSL}^{tot}}{2-\alpha} = 2 \cdot (1+\beta) \cdot N_{TSL}^{tot} \quad (12)$$

Therefore the utilization of the TSLs by the OSC users can be expressed as a function of OSC user penetration:

$$\beta = \frac{\alpha}{2-\alpha} \quad (13)$$

FIGURE 5 shows the physical TSL utilization for the OSC and HR users as a function of the OSC penetration, i.e., the level of the TSL occupation as a function of the percentage of the SAIC capable handset of the all mobiles in the investigated area.

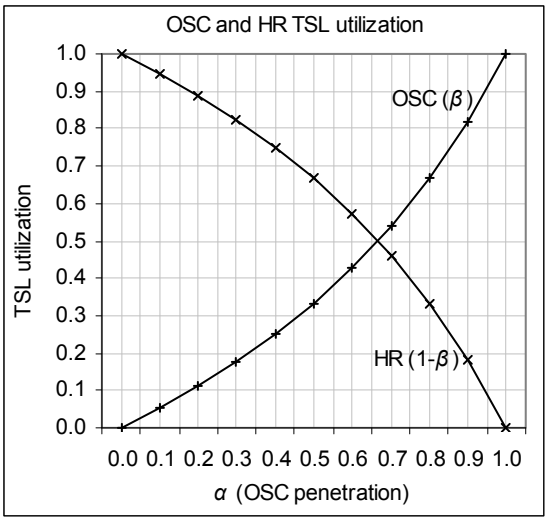

FIGURE 5. The TSL utilization for the OSC and HR calls as a function of the OSC penetration.

One point of interest of FIGURE 5 is the SAIC handset penetration of 50%, which indicates that the OSC paired connections utilize 33% of the physical TSL capacity of the cell, the rest being occupied by HR users. Another point of interest is the breaking point where both HR and OSC utilize the same amount of TSLs. The graph shows that it is found at 67% of OSC penetration.

It should be noted that the calculation is valid within the functional coverage area where OSC can be used, i.e., where the received power level is high enough. For the areas outside the OSC coverage, HR and FR modes are assumed to function normally with their respective ranges of received power levels indicated in [15].

B. The effect of OSC on the number of users per TSL

As the number of the OSC and HR users is known as a function of α, we can create a function that expresses the usage of a single TSL in terms of the number of users served. It is clear that the values of the served users oscillates within the range of [2, 4], lowest value indicating 100% HR, and highest value representing the 100% DHR OSC penetration.

The number of the users per TSL in a cell that contain mixed HR and OSC users can be obtained by utilizing (10) and (11):

$$\frac{N_{MS}^{tot}}{N_{TSL}^{tot}} = 2 \cdot \left(1 + \frac{\alpha}{2-\alpha}\right) \quad (14)$$

FIGURE 6 shows the number of users per TSL as a function of the OSC penetration α. As can be noted, the extreme value of 4 is a result of OSC penetration of 100%.

As an example, the 50% OSC penetration level provides an offered capacity for about 2.67 users (which is a mix of OSC and HR users in average) per timeslot. It is again assumed that the OSC functionality can be utilized over the whole investigated area, meaning that the cell border area of the GSM coverage is not considered in this analysis.

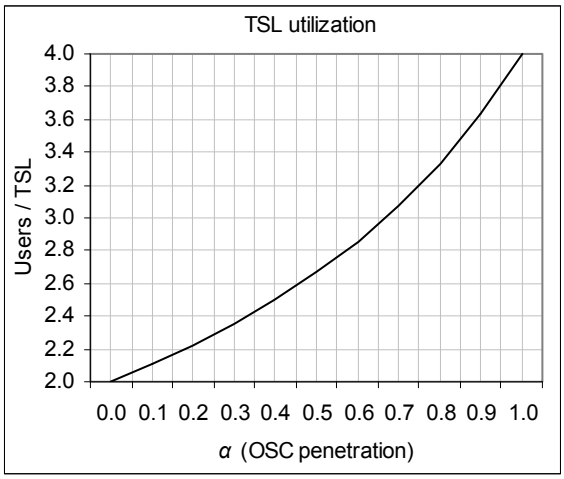

FIGURE 6. The number of users per TSL as a function of the OSC penetration.

C. *The effect of OSC on blocking rate*

The original situation of the fully occupied cell with only HR users present, i.e., when OSC is not activated, can be taken as a reference also for the following analysis. Assuming that the blocking rate of the GSM HR cell in busy hour is B, we can estimate its change via the well-known Erlang B [16] after OSC has been activated:

$$B(N) = \frac{\frac{A^N}{N!}}{\sum_{n=0}^{N} \frac{A^N}{n!}} \tag{15}$$

Term B is the blocking rate (% of the blocked calls compared to the number of whole attempts), N is the available amount of time slots, and A is the product of the average call density and average time of reservation, i.e., the offered load.

As it is not possible to solve the equation of offered traffic analytically, it can be utilized in a recursive format:

$$\begin{cases} B(0) = 1 \\ B(N) = \dfrac{AB(N-1)}{N + AB(N-1)} \end{cases} \tag{16}$$

Furthermore, the offered traffic (Erl) can be expressed as:

$$\bar{x} = A \cdot (1 - B) \tag{17}$$

We can establish a reference case with OSC 0% in the following way. The *B(N)*[OSC = 0%] can be set to 2%. This means that, e.g., in the case of 7 traffic TSLs for FR GSM, the respective offered load A = 2.94 Erl and the offered traffic is $\bar{x}$ = 2.88 Erl. The proportion of the offered traffic over the whole timeslot capacity $\bar{x}$ / TSL_{tot} = 0.41 Erl/TSL. If HR codec is utilized, there is double the amount of users served within the same TSL number. This can be expressed in Erlag B formula by marking the available radio resources as 14, which results A = 8.21 Erl and $\bar{x}$ = 8.04 Erl. The $\bar{x}$ / TSL_{tot} is now 1.15 Erl/TSL, i.e., FR TSL. The difference between these figures shows the Erlag B plus HR gain, i.e., the more there is available capacity, the more efficiently the calls can be delivered with the same blocking rate.

When the OSC functionality is activated and the same blocking rate is maintained, the available resources with the same hardware is now 4·7 = 28 for the *B(N)*[OSC = 100%], i.e., when α = 1. The $\bar{x}$ is now 19.75, and the efficiency 2.82 Erl/TSL, i.e., FR TSL. This shows one of the benefits of OSC as it increases clearly the capacity efficiency via the Erlang B gain if the same amount of hardware is maintained.

If instead the amount of users is kept the same, the additional capacity that is liberated via the more efficient usage of TSLs via OSC can be removed partially or totally. This provides the basis for 3G re-farming if the operator has both 2G and 3G licenses.

With a lower amount of timeslots, the same number of users can still be served with the same or lower blocking rate like FIGURE 6 indicates. The blocking rate depends on the usage of the TSLs for OSC, i.e., on β, which can be expressed as a function of α as shown in (13).

D. *The effect of OSC on the TSL and TRX reduction*

It is possible to investigate the dependency of the number of users and Erlang B formula's offered traffic as a function of the OSC penetration. In order to carry out this part of the study, an Erlang B table was created by utilizing (15) and (16).

A case example with a blocking rate of 2.0% was selected. A table of 1–200 TSLs was created as a basis for the analysis. FIGURE 7 summarizes the behavior of the channel utilization. It can be seen that the performance of the cell increases due to the Erlang B gain, along with the OSC penetration growth compared to the original proportion of the HR capable users.

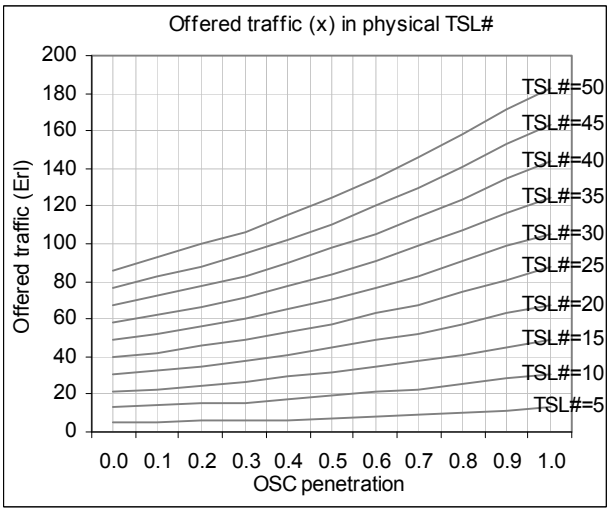

FIGURE 7. Offered traffic as a function of the OSC penetration, when the maximum number of the available time slots is 50 and B = 2%.

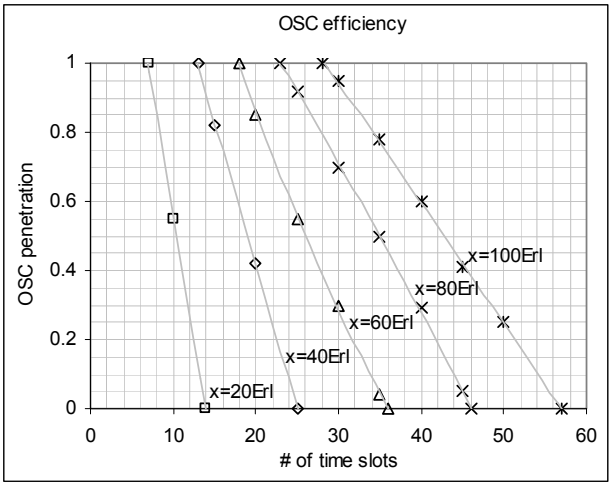

FIGURE 8. The required time slot number with B = 2% can be observed as a function of the OSC capable user penetration.

Next, an analysis of the effect of the SAIC handset penetration on the total reduction of the time slot number is presented. The calculation can be made by assuming that the offered traffic level $\bar{x}$ and the call blocking rate B are maintained in the original level.

FIGURE 8 summarizes the analysis carried out for 20–100 Erl of offered traffic. FIGURE 8 can be interpreted in such a way that when the OSC penetration grows, the needed number of TSLs with the same blocking rate (originally 2%) is now lower.

According to the basic behavior of the Erlang B model, the effect is logically strongest for the higher capacity cells. This can be noted especially from the highest investigated offered traffic class of 100 Erl, which requires only half of the timeslots when OSC penetration is 100%.

The effect of OSC can be seen in FIGURE 9, which shows the analysis for the required number of TRXs for a set of offered traffic classes (Erl) when the OSC capable SAIC handset penetration is known.

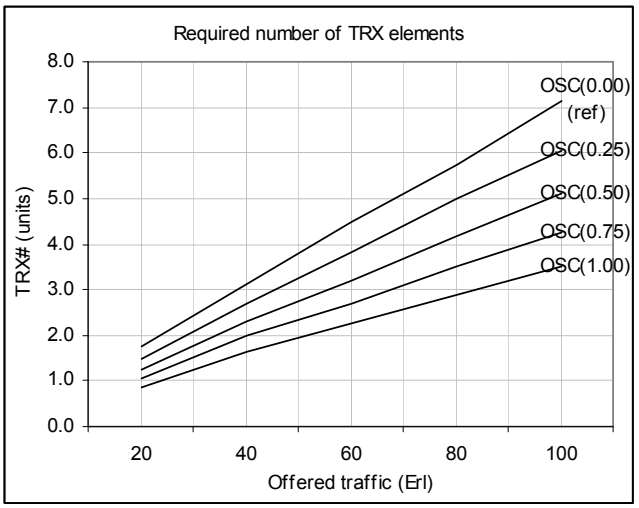

FIGURE 9. The effect of the OSC penetration on the required amount of TRXs when the blocking rate B is kept the same (2%).

The assumption in this case is that each TRX contains 8 traffic channels. It is now possible to interpret the benefit of OSC in terms of the transceiver units. Table I summarizes the calculation as a function of TRX number.

TABLE 1. The estimation of the needed TRX element number as a function of the OSC penetration, when the blocking probability B=2%.

$\bar{x}$ (Erl)	OSC penetration				
	0.00	**0.25**	**0.50**	**0.75**	**1.00**
20	1.8	1.5	1.3	1.1	0.9
40	3.1	2.7	2.3	2.0	1.6
60	4.5	3.8	3.2	2.7	2.3
80	5.8	5.0	4.2	3.5	2.9
100	7.1	6.1	5.1	4.3	3.5

TABLE 1 indicates that the benefit of OSC starts to be significant when the original BTS contains at least 4 TRX elements (per sector or in omni-radiating site). In that case, already a relatively low OSC penetration of 25% provides a possibility to remove a complete TRX element (i.e., one frequency block of 200 kHz) from the cell, yet still keeping the blocking rate below or the same as was observed originally, which is 2% in this example. If this capacity is removed, it can be utilized for the re-farming of 3G frequencies. Alternatively, if no TRX units are removed, the offered capacity can be utilized more efficiently for parallel packet data via the lower circuit switched call blocking rate. There are thus various different network evolution scenarios available due to OSC.

FIGURE 10 summarizes the amount of TRXs (assuming that each offers 8 physical traffic TSLs) that can be removed from the site depending on the OSC penetration and the offered traffic in such a way that the blocking rate would not change from the original 2 % figure. It should be noted that a small part of the TSLs are used also for signaling, and that each TRX unit is a physical 8-TSL equipment, so only integer values rounded up should be considered in the interpretation of the number of TRXs.

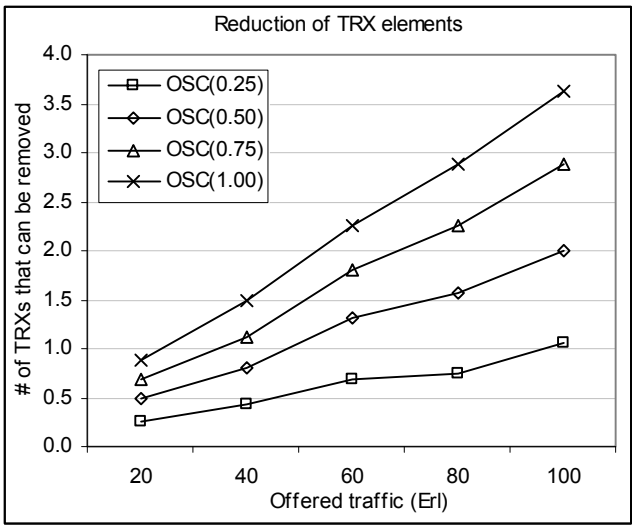

FIGURE 10. The effect of OSC on the reduction of TRX elements.

The presented analysis provide a base for the GSM network re-dimensioning in the following scenarios:

1) In the case of still growing GSM traffic, the estimation of the already existing penetration of SAIC terminals when the OSC feature is activated, as well as the prediction of the SAIC penetration development within the forthcoming years gives a possibility to adjust the radio capacity plans. This means that the otherwise required TRX extensions can be postponed or rejected as long as the blocking rate can be maintained in the allowed level with OSC.

2) In the case of stabilized or lower GSM traffic, the same blocking rate can be maintained with a lower amount of the TRX units. This liberated bandwidth can be reused for the delivery of the growing 3G traffic in the same frequency band, if available for the operator, which makes the frequency re-farming more fluent with OSC.

IV. OSC Radio Performance Analysis

A. Methodology for the analysis

The laboratory environment consisted of Base Station Sub system (BSS) and Network and Switching Sub-system (NSS) with functional elements (Base Transceiver Station BTS, Base station Controller BSC, Mobile Switching Centre MSC and Home Location Register HLR) as shown in Figure 11. The Abis interface was based on the IP emulation. The BTS was located in Madrid, Spain, and BSC in Finland. The voice calls were established only within the test network. Discontinuous Transmission (DTX) and Frequency Hopping (FH) were disabled during the measurement data collection.

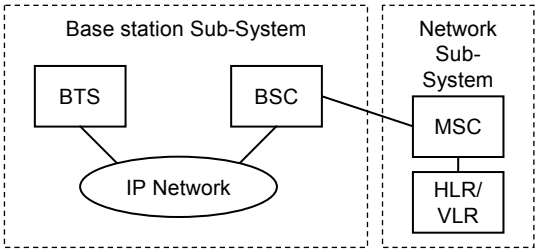

Figure 11. The laboratory setup consisted of a functional GSM network with a single radio cell.

The test network consisted of one cell in the indoors. The link budget was dimensioned by using adjustable attenuators and minimal TRX output power, which resulted in a cell radius of about 40 meters. The indoor radio propagation conditions provided nearly line of sight, with light wall obstacles. This setup represents a noise-limited environment within the whole functional received power level range of GSM.

For the evaluation of the radio performance, the quality level Q and received power level P_{RX} were correlated and stored in Slow Associated Control Channel (SACCH) frame intervals of 480 ms during the active voice calls. The correlated Q_n values with n = 0...7 and P_{RXm} categories with m = 0...5 were collected to a matrix. Table 2 presents the equivalence of the Q levels and bit error rate (BER), and Table 3 shows the P_{RX} categories in terms of dBm ranges [15].

The values for the Carrier-to-Noise ratio (C/N) are based on the thermal noise level and terminal's noise figure. The value for the noise floor can be estimated by applying the formula:

$$P_n = 10\log_{10}\left(k_B T B \cdot 10^3\right) dBm = -174 dBm/Hz + 10\log_{10}(B) Hz \quad (18)$$

where k_B is Boltzmann's constant ($1.38 \cdot 10^{-23}$ J/K), T is the temperature (290 K is assumed) and B is the bandwidth in Hz. For a single GSM frequency channel of 200 kHz, the thermal noise level is thus −120.98 dBm. The values of Table 3 contain also the receiver noise power of about 3 dB, resulting in total noise level N of −118 dBm.

The OSC functionality was set up to the BTS and BSC by utilizing non-commercial R&D software. DHR mode of OSC was utilized in a single TSL with minimally correlating training sequences.

Table 2. Mapping of quality categories (Q) and Bit Error Rates (BER).

Q_n category	BER (%)
n=0	[0.0, 0.2]
n=1	[0.2, 0.4]
n=2	[0.4, 0.8]
n=3	[0.8, 1.6]
n=4	[1.6, 3.2]
n=5	[3.2, 6.4]
n=6	[6.4, 12.8]
n=7	[12.8, 100]

Table 3. P_{RX} categories and respective Carrier-to-Noise ranges.

P_{RXm} category	P_{RX} (dBm)	C/N (dB)
m=5	[−38, −69]	[49, 80]
m=4	[−70, −79]	[39, 48]
m=3	[−80, −89]	[29, 38]
m=2	[−90, −94]	[24, 28]
m=1	[−95, −99]	[19, 23]
m=0	[−100, −110]	[8, 18]

B. Laboratory tests with SAIC handsets

The data collection was carried out over the functional coverage area by applying BSC measurement called RxLevel Statistics. SAIC terminals were used for the test calls. The collection was done in systematic manner by moving the terminals approximately 0.5 m/s with a test platform.

The correlated (Q, P_{RX}) matrix was collected for both OSC and reference GSM HR calls. It should be noted that the testing was done only for one physical TSL whilst the other traffic TSLs were blocked. As the environment was noise-limited and no inter-TSL interferences were present, this represents a fully loaded cell. The interval of the (Q, P_{RX}) matrices was 15 minutes.

Figure 12 shows the principle of the data collection, which was carried out in three different phases within high, medium and low ranges of received power levels. This method was applied to the investigations in order to collect the data over the P_{RX} categories in as uniform manner as possible.

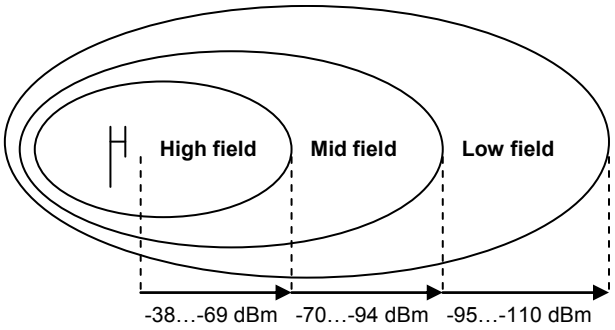

FIGURE 12. The measurement data were collected in three phases, within high, mid and low field (values of P_{RX} in dBm).

C. Laboratory results

The correlated (Q_n, P_{RXm}) results can be organized to a matrix format in such a way that the elements $v_{i,j}$ correspond to the number N of the samples of Q_{8-i}, where i=0,1,...,8, and P_{RXj-1}, with j=0,1,...,5, is indicated as $N(Q_n, P_{RXm})$. The result of (Q_0, P_{RX0}) represents thus the value of the matrix element $v_{8,1}$ and (Q_1, P_{RX1}) corresponds to the element $v_{7,1}$. The last result of (Q_7, P_{RX5}) is found in the element $v_{1,6}$. The following format clarifies the idea.

$$M = \begin{bmatrix} v_{1,1} & v_{1,2} & \cdots & v_{1,6} \\ v_{2,1} & \ddots & & \\ \vdots & & \ddots & \\ v_{8,1} & & & v_{8,6} \end{bmatrix} = \begin{bmatrix} N(Q_7,P_0) & \cdots & \cdots & N(Q_7,P_5) \\ N(Q_6,P_0) & \ddots & & \\ \vdots & & \ddots & \\ N(Q_0,P_0) & & & N(Q_0,P_5) \end{bmatrix}$$

The following matrices M_{GSM} and M_{OSC} presents the normalized results for GSM and OSC laboratory tests, respectively. Each matrix element represents the percentage of the number of samples for that Q and P_{RX} compared to the total number of samples.

$$M_{GSM} = \begin{bmatrix} 1.70 & 0.00 & 0.00 & 0.00 & 0.00 & 0.00 \\ 2.67 & 0.02 & 0.02 & 0.01 & 0.00 & 0.00 \\ 3.57 & 1.31 & 0.95 & 0.39 & 0.08 & 0.02 \\ 3.81 & 1.96 & 0.71 & 0.23 & 0.02 & 0.03 \\ 2.97 & 1.69 & 0.58 & 0.30 & 0.04 & 0.03 \\ 1.11 & 1.34 & 0.63 & 0.32 & 0.03 & 0.03 \\ 0.66 & 0.66 & 0.18 & 0.23 & 0.06 & 0.02 \\ 1.81 & 5.33 & 10.35 & 14.13 & 11.47 & 28.56 \end{bmatrix}$$

$$M_{OSC} = \begin{bmatrix} 4.44 & 0.03 & 0.00 & 0.00 & 0.00 & 0.00 \\ 2.85 & 5.09 & 0.01 & 0.01 & 0.00 & 0.00 \\ 0.00 & 5.36 & 1.93 & 0.16 & 0.00 & 0.03 \\ 0.00 & 0.80 & 6.95 & 0.70 & 0.00 & 0.05 \\ 0.00 & 0.07 & 6.53 & 1.42 & 0.02 & 0.04 \\ 0.00 & 0.00 & 4.19 & 0.99 & 0.07 & 0.05 \\ 0.00 & 0.00 & 1.97 & 1.19 & 0.05 & 0.07 \\ 0.02 & 0.00 & 2.07 & 18.65 & 24.24 & 9.92 \end{bmatrix}$$

In the original GSM mode and with full load of a single TSL, a total of two HR users consume the whole physical TSL. In the OSC mode, in turn, a total of 4 DHR users utilizes the physical TSL in the fully loaded TSL.

The Q_n and P_{RXm} results were collected in three phases, each lasting 15 minutes. One area is characterized as a strong field with main part of the results occurring in P_{RX} categories of P_{RX5} and P_{RX4}. The second represents medium field with values of P_{RX3} and P_{RX2}, and the third area represents low field with values belonging to P_{RX1} and P_{RX0}. The results were then combined in order to present the matrix of the complete field.

All the measurement data samples were collected as uniformly as possible by moving the platform in a constant speed. The data collection in the lowest field was done by observing the Radio Link Timer (RLT) parameter value directly in the mobile phone's engineering mode channel display. When the field reached the critical level, there occurred SACCH frame errors and the retransmission parameter value started to decrease from the original value of 20 towards 0. Before the zero-value was reached (which drops the call), the mobile was moved to the better field in order to raise the value back to 20 without breaking the connection.

There were a total of 20,383 and 19,399 samples collected during the GSM HR and OSC modes, respectively. In average, there is thus more than 400 samples per matrix element, which results in an average margin error Err[95%] = 0.98 / √(400) = 4.9% with 95% confidence level per each matrix element. Table III shows the Err[95%] for each P_{RX} category.

TABLE 4. The error margin in % of the samples of each P_{RXm} category with 95% confidence level.

Mode	P_{RX0}	P_{RX1}	P_{RX2}	P_{RX3}	P_{RX4}	P_{RX5}
HR	1.6	2.0	1.9	1.8	2.1	1.3
OSC	2.5	2.0	1.4	1.4	1.4	2.2

D. OSC Radio Performance Model

Based on the analysis presented previously, a comparison of the matrices can be now performed. GSM HR matrix M_{GSM} can be selected as a reference in order to produce a matrix M_{diff}, which indicates the difference or change of the original correlated (Q, P_{RX}) distribution in %-units due to the OSC mode. The matrix is:

$$M_{diff} = M_{GSM} - M_{OSC} \tag{19}$$

$$M_{diff} = \begin{bmatrix} -2.74 & -0.03 & 0.00 & 0.00 & 0.00 & 0.00 \\ -0.18 & -5.07 & 0.00 & -0.01 & 0.00 & 0.00 \\ +3.57 & -4.05 & -0.98 & +0.23 & +0.08 & -0.02 \\ +3.81 & +1.16 & -6.25 & -0.46 & +0.01 & -0.02 \\ +2.97 & +1.61 & -5.95 & -1.12 & +0.01 & -0.01 \\ +1.11 & +1.34 & -3.56 & -0.67 & -0.05 & -0.02 \\ +0.66 & +0.66 & -1.79 & -0.96 & +0.01 & -0.06 \\ +1.79 & +5.33 & +8.28 & -4.51 & +12.77 & +18.65 \end{bmatrix}$$

It can be noted that in the original M_{GSM}, there are all quality classes $Q_0 \ldots Q_7$ present in the lowest field, i.e., in P_{RX0} category, whilst M_{OSC} produces samples only to the quality classes Q_6 and Q_7 in the same field. It can be seen that the collection of samples for different P_{RX} levels is not uniform, indicating that the data collection happened slightly unequally in different fields, in addition to the fact that the ranges associated with each P_{RX} are different. This makes the comparison of the matrices challenging.

In order to cope with this issue, the result matrices can be normalized over each P_{RXm} category (that is by column) instead of the total number of the collected samples, in the following way:

$$M'_{GSM} = \begin{bmatrix} 9.29 & 0.00 & 0.00 & 0.00 & 0.00 & 0.00 \\ 14.6 & 0.13 & 0.12 & 0.03 & 0.00 & 0.00 \\ 19.5 & 10.7 & 7.07 & 2.48 & 0.71 & 0.05 \\ 20.8 & 16.0 & 5.27 & 1.49 & 0.13 & 0.09 \\ 16.2 & 13.7 & 4.34 & 1.92 & 0.31 & 0.11 \\ 6.08 & 10.9 & 4.69 & 2.05 & 0.22 & 0.09 \\ 3.63 & 5.40 & 1.35 & 1.45 & 0.49 & 0.05 \\ 9.88 & 43.3 & 77.16 & 90.6 & 98.2 & 99.6 \end{bmatrix}$$

$$M'_{OSC} = \begin{bmatrix} 60.7 & 0.26 & 0.00 & 0.00 & 0.00 & 0.00 \\ 39.0 & 44.8 & 0.06 & 0.06 & 0.00 & 0.00 \\ 0.00 & 47.2 & 8.15 & 0.68 & 0.02 & 0.34 \\ 0.00 & 7.04 & 29.4 & 3.01 & 0.02 & 0.48 \\ 0.00 & 0.65 & 27.6 & 6.13 & 0.10 & 0.43 \\ 0.00 & 0.04 & 17.7 & 4.29 & 0.30 & 0.48 \\ 0.00 & 0.00 & 8.32 & 5.14 & 0.20 & 0.72 \\ 0.27 & 0.00 & 8.75 & 80.7 & 99.36 & 97.5 \end{bmatrix}$$

Now, the difference can be calculated as:

$$M'_{diff} = M'_{GSM} - M'_{OSC} \tag{20}$$

The following matrix presents the result in %.

$$M'_{diff} = \begin{bmatrix} +51.5 & +0.26 & 0.00 & 0.00 & 0.00 & 0.00 \\ +24.4 & +44.7 & -0.05 & +0.03 & 0.00 & 0.00 \\ -19.5 & +36.5 & +1.08 & -1.80 & -0.69 & +0.28 \\ -20.8 & -8.91 & +24.1 & +1.53 & -0.11 & +0.39 \\ -16.2 & -13.1 & +23.3 & +4.22 & -0.21 & +0.33 \\ -6.08 & -10.8 & +13.0 & +2.24 & +0.08 & +0.39 \\ -3.63 & -5.40 & +6.97 & +3.68 & -0.28 & +0.67 \\ -9.61 & -43.3 & -68.4 & -9.90 & +1.21 & -2.07 \end{bmatrix}$$

It can be seen from the matrices that the proportion of quality classes Q_7 and Q_6 is higher in OSC than in GSM HR.

FIGURE 13 shows the impact of OSC on the quality level per each P_{RX} category. The most affected categories are P_{RX0}, P_{RX1} and P_{RX2} as they include more lower quality values.

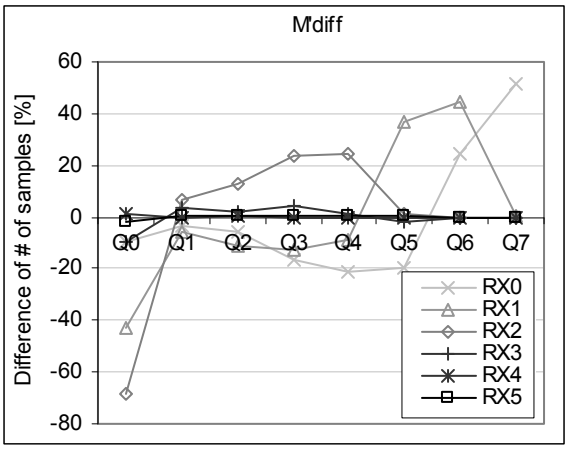

FIGURE 13. The M'diff presents the change in the distribution of the correlated Q and P_{RX} caused by OSC when HR is the reference.

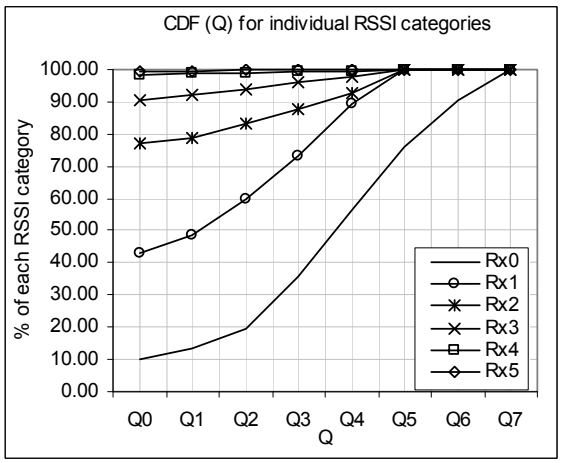

FIGURE 14. CDF of the GSM HR analysis, scaled individually for each P_{RX} category.

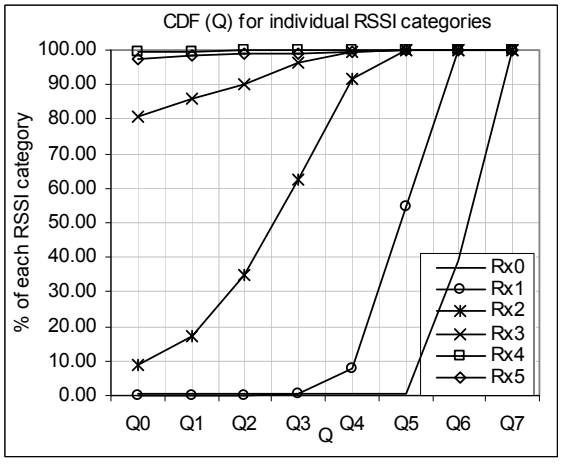

FIGURE 15. CDF of the OSC analysis, scaled individually for each P_{RX} category.

FIGURE 14 and FIGURE 15 show the difference in the Q class behavior. In GSM HR, the lowest P_{RX} has samples over all the Q classes whilst OSC only causes samples for Q_6 and Q_7.

The introduction of OSC feature causes each CDF to shift towards the higher Q classes corresponding to higher BER. This indicates that the useful coverage area produced via the OSC mode is smaller than the one produced by HR.

1) Scenario 1: Difference of the radio quality in a fully loaded GSM HR and OSC cell

TABLE 5 summarizes the laboratory test analysis in CDF, showing the differences between HR and OSC per P_{RX} category. As can be noted, the Q_5, i.e., BER in the interval [3.1%, 6.4%] can be reached with HR between P_{RX0} and P_{RX1} [–95, –110 dBm]. According to Table III, the OSC moves the C/N requirement higher, and the Q_5 can now be found between P_{RX1} and P_{RX2} [–90, –99 dBm].

TABLE 5. The 95 % Q criterion analysis for the GSM HR calls.
* Note: When the Q_0 value is achieved more than 95 % of the time, the corresponding %-value is shown in brackets.

P_{RX} category	Q value for GSM HR (reference)	Q value for OSC / difference with GSM HR (%-units)
P_{RX0}	6.5	6.9 / –0.4
P_{RX1}	4.5	5.9 / –1.4
P_{RX2}	4.3	4.4 / –0.1
P_{RX3}	2.5	2.8 / –0.3
P_{RX4}	0.0* (98.1 %)	0.0* (97.5 %) / 0.0 (–0.6 %-units)
P_{RX5}	0.0* (99.6 %)	0.0* (99.4 %) / 0.0 (–0.2 %-units)

It can be assumed that the practical threshold for the GSM call is at quality level of Q_4, corresponding to a BER in the range [1.6, 3.2]. FIGURE 16 shows the CDF of the combined P_{RX} classes as a function of the Q, indicating that the Q_4 is at 89.5% for GSM HR, and at 80.0% for OSC over the whole investigated area A_{GSM} in this specific case.

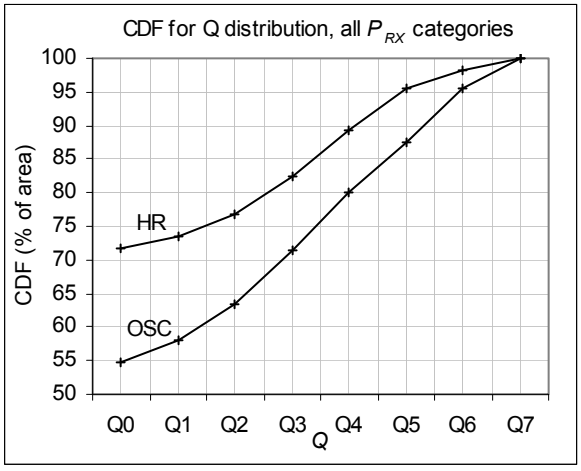

FIGURE 16. The HR and OSC coverage.

The CDF of HR and OSC indicates the presence of different Q classes during the measurement, which shows the percentage of Q classes in the investigated area. The effect of OSC can now be observed based on Q_4:

$$A_{change}[\%] = 100\frac{A_{HR} - A_{OSC}}{A_{HR}} = 100\left(1 - \frac{A_{OSC}}{A_{HR}}\right) \approx 10.6\% \quad (21)$$

where A_{change} indicates how much the useful coverage area of OSC is smaller compared to the HR mode. The radius for the OSC mode is reduced from the HR mode by:

$$r_{change}[\%] = 100 \cdot \frac{r_{HR} - r_{OSC}}{r_{HR}} = 100 \cdot \left(1 - \frac{r_{OSC}}{r_{HR}}\right) = 100 \cdot \left(1 - \sqrt{\frac{A_{OSC}}{A_{HR}}}\right) \approx 5.5\% \quad (22)$$

As the OSC brings up to 100% capacity enhancement compared to the GSM HR, the benefit of OSC is clear even with this level cell size reduction.

In practice, the original cell size remains as determined by the GSM FR and HR limits for the C/N and C/I levels. In other words, when the OSC feature is activated, the cell contains OSC, HR and FR coverage regions. The FR proportion remains the same also after the activation of OSC, but HR region is divided into OSC and HR regions. The final size of these depends mainly on the original overlapping portions of the neighboring cells and the criteria of the intra/inter-cell handover algorithms.

Furthermore, the OSC proportion depends also on the time slot usage by OSC, β, which in turn depends on the OSC capable handset penetration α.

2) Scenario 2: Only OSC (SAIC) handset penetration is known

In a practical GSM network, there is a certain penetration of OSC capable terminals in the investigated field. When OSC is activated, there are legacy terminals that are capable of functioning only with the previous GSM codecs (FR, HR, AMR), and SAIC terminals that are also capable to function in the DHR mode.

It is thus important to take the SAIC terminal penetration into account when modeling the effect of OSC in the field. The M'_{GSM} and M'_{OSC} presented previously show the correlated distribution of (Q, P_{RX}) in a fully loaded situation, i.e., when all the time slots are occupied either by GMS HR or OSC users. We can still utilize this assumption of fully loaded cell in order to find the limits of the effect. Let's assume the SAIC handset penetration is α of all the terminals in the investigated area. As the OSC DHR utilizes single TSL for a total of 4 users whilst GSM HR can multiplex two users in the same TSL, the TSL capacity related scaling factor is needed for the performance model.

In a typical case, there are 2 or more TRXs per cell in sub-urban areas, and 4 or more in dense city environment. The TSL utilization of the OSC vs. HR can be estimated by α. The TSL utilization factor β for the OSC TSL occupancy

in a fully loaded cell as a function of the OSC mobile terminal penetration can be formulated as presented in [1]:

$$\beta = \frac{\alpha}{2-\alpha} \tag{23}$$

Now, when M'_{GSM}, M'_{diff} and OSC penetration α are known, the M'_{OSC} can be obtained by scaling the original GSM matrix element-wise. We can donate the elements of the matrix M'_{GSM} as $v_{m,n}^{GSM'}$ and the elements of the matrix M'_{OSC} as $v_{m,n}^{OSC'}$. The scaling between these corresponding elements can be assumed to be linear according to the principle of the linear interpolation function:

$$y = kx + b \quad , \tag{24}$$

where $\{k \in \mathbb{R} | 0 \le k \le 1\}$ and represents the coefficient in x-axis of the physical TSL usage, i.e.:

$$k = v_{m,n}^{OSC'} - v_{m,n}^{GSM'} \tag{25}$$

Term b is the value of y when x = 0, i.e., it equals to $v_{m,n}^{GSM'}$. Term x represents the usage of the TSLs for the OSC:

$$x = \beta \tag{26}$$

The scaling of each element for the partially loaded OSC cells can thus be done as follows:

$$y_{m,n} = \left(v_{m,n}^{OSC'} - v_{m,n}^{GSM'}\right) \cdot \beta + v_{m,n}^{GSM'} \tag{27}$$

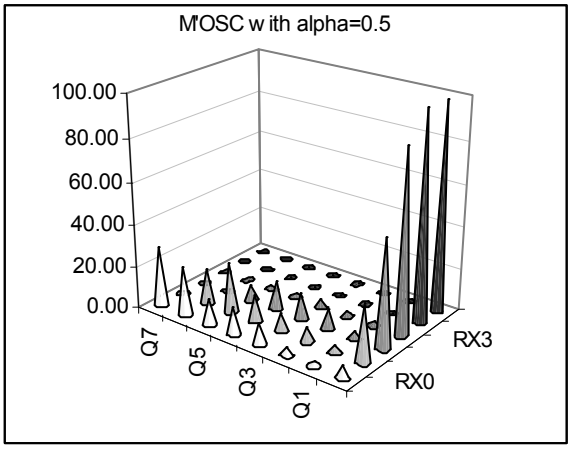

FIGURE 17. An example of the expected (Q, P_{RX}) distribution (normalized over each RXlevel category) when OSC user penetration α is 50% and the OSC TSL usage B is 37.5%.

M'_{GSM} and M'_{OSC} obtained from the laboratory can be utilized directly, and the estimate of the new M'_{OSC} (α) can be thus constructed by interpolating linearly the matrix values element-by element basis.

The usage of the laboratory results is most accurate in environment that contains approximately same type of radio channel, i.e., in noise-limited environment with almost line-of-sight and light proportion of Rayleigh fading. If the radio channel differs considerably from the laboratory, Scenario 3 should be considered instead. This means that the case results presented in this paper might vary depending, e.g., on the level of the co-channel and adjacent channel interferences as well as on the type of multi-path propagation characteristics in the investigated area.

3) Scenario 3: OSC (SAIC) handset penetration and new M'_{GSM} are known

When the new M'_{GSM} is known, showing the correlated (Q_n, P_{RXm}) matrix for HR calls, it can be assumed that the new M'_{OSC} is possible to construct by applying the M'_{diff} that was obtained from the laboratory. The assumption is that the OSC feature performance is independent of the radio conditions, i.e., the reference M'_{GSM} obtained from the laboratory already contains the radio channel related performance, whilst M'_{OSC} includes this same radio performance effect and an additional OSC performance specific performance. Assuming this is applicable in varying radio conditions, the new M'_{OSC} can be constructed by taking into account the OSC penetration:

$$M'_{OSC} = M'_{GSM} + \beta \cdot M'_{diff} \tag{28}$$

As explained in scenario 2, the activation of OSC is seen within the HR coverage area, the FR area staying unchanged. The utilization of the OSC compared to the original HR region can now be interpreted from the practical measurements or by taking again the Q_4 criterion as a basis. Also another value of the quality classes can be utilized, if that corresponds to the OSC pairing and un-pairing criteria of the OSC algorithm.

V. COMPLETE OSC MODEL

The strength of the developed model is that it requires only few and basic inputs, which are: 1) Rx Level Statistics tables before the OSC functionality is activated; 2) estimation of the OSC capable penetration in the initial phase of the OSC activation; and 3) optionally the percentage of the utilized HR and FR codecs.

A. OSC model process

FIGURE 18 shows the complete process of the model. The model processes the input data in such a way that the expected (Q,P_{RX}) matrix is formed based on the measured and correlated (Q, P_{RX}) table element-by-element according to (27). By default, the scaling of each element can be done by utilizing the already formed difference matrix. It should be noted that the presented difference matrix is valid for the noise-limited environment, so new difference matrix might be needed for the interference-limited environment.

The output of the model indicates the proportion of the OSC usage as a function of the OSC capable handset penetration, with the capacity gain that can be expressed in

terms of increased offered load/traffic or of the possibility to reduce TRX elements. The radio performance result is based on the analysis of the changed *C*/*I* or *C*/*N* distributions.

When the complete model is applied in the investigation of a realistic GSM network, the steps described in FIGURE 18 can be taken into account for solving first the impact on the radio performance, i.e., on the changes of the quality.

The actual capacity gain depends on the radio performance, i.e., which proportion of the GSM call can be utilized for the OSC, and on the OSC penetration, i.e., what share of the handsets can take the advantage of the usable coverage area for the OSC. The estimate of the performance change due to the activation of OSC would be made based on the pre-formed difference matrices and the SAIC penetration.

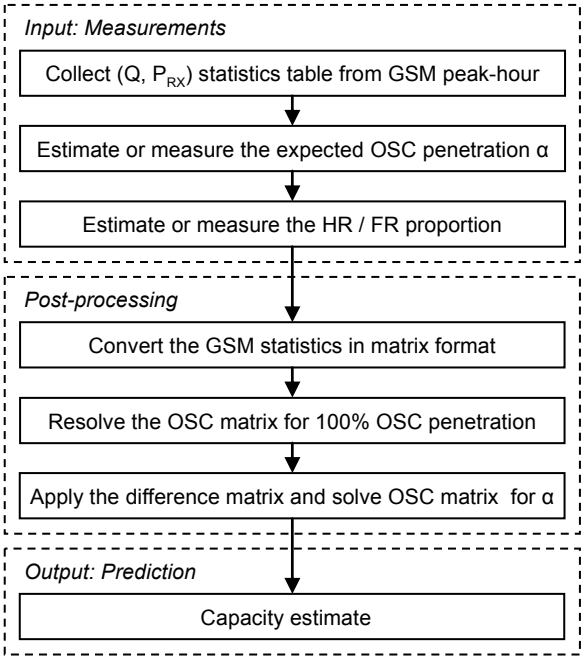

FIGURE 18. The process chart of the OSC model usage.

When the Rx level statistics table of GSM is measured from the field (i.e., the table without OSC feature activated), it can be assumed that the corresponding expected Rx level statistics table for the OSC is possible to construct by applying the correction curves that were obtained from the laboratory as shown in FIGURE 13. The assumption is that the OSC feature performance is independent of the radio conditions, i.e., the reference table of GSM obtained from the laboratory already contains the radio channel related performance, and that the OSC table includes this same radio performance effect and an additional OSC performance specific performance. Assuming this is applicable in varying radio conditions, the new OSC table can be constructed by taking into account the OSC penetration:

$$M'_{OSC} = M'_{GSM} + \beta \cdot M'_{diff} \quad , \tag{29}$$

where M'_{OSC} is the matrix format for the new OSC Rx level statistics table, M'_{GSM} is the matrix of the measured GSM Rx levels statistics table in the field, and M'_{diff} is the correction matrix obtained from the laboratory measurements. The practical way of constructing the OSC Rx level table is to utilize the β factor element-by-element basis for scaling first each of the difference matrix elements. Then, the difference matrix is utilized to scale the GSM Rx level statistics table element-by-element basis.

B. Process steps

The complete OSC model considers the radio performance, or changes of the performance due to the OSC activation, as well as the resulting capacity gain. The steps for the investigation of the OSC impact are:

Step 1: Storing of the Rx Level statistics measurement and codec utilization measurement via BSC. This gives the reference for the GSM performance without OSC.

From the codec utilization measurement, also the estimate of what is the utilization (percentage) of HR and FR codecs can be included. That information gives the equivalence of the original HR-FR division also area-wise as shown in FIGURE 19.

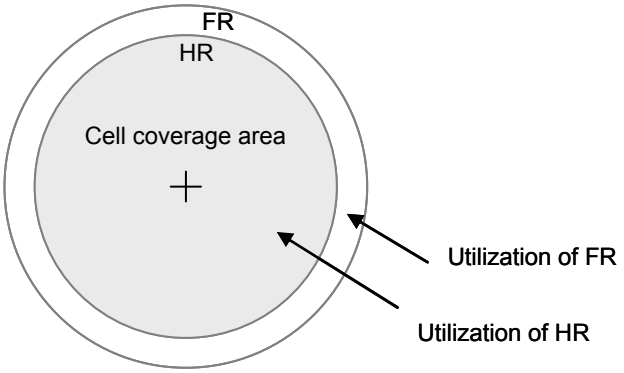

FIGURE 19. The original division of the FR and HR mode utilization before the OSC feature has been activated.

The investigation of the utilization of the codecs can be done for any time of the traffic, but the peak hour as criterion is recommended in order to collect as much data as possible in the given time window, and to make sure that the behavior of the effect of OSC on the capacity is done in the extreme conditions that represents the practical limit for the gain. In order to increase the accuracy of the estimate, the Rx level statistics measurement for the storing of the correlated Q and P_{RX} table can be done at the same time as the codec division.

Step 2: Estimation of the OSC capable SAIC handset proportion in the field, i.e., the factor α. The estimate can be carried out via the network statistics that is based on an IMEI (International Mobile Equipment Identity) analysis, which is correlated with the database of the models that support SAIC. The estimate can also be done based on the sales statistics, or other practical "best-effort" estimate. Based on this information, the average TSL utilization for the OSC capable handsets can be estimated by using (23).

Step 3: Estimation of the capacity regions assuming the OSC DHR functions within a part of the HR region. The FR region can be assumed to work unchanged, as the situation

was before the OSC activation. The criterion for the OSC percentage can be selected as presented in FIGURE 16, i.e., based on the Q_4 level in CDF of the area. If the practical implementation of the OSC pairing and un-pairing is based on the other Q levels, that can be utilized instead.

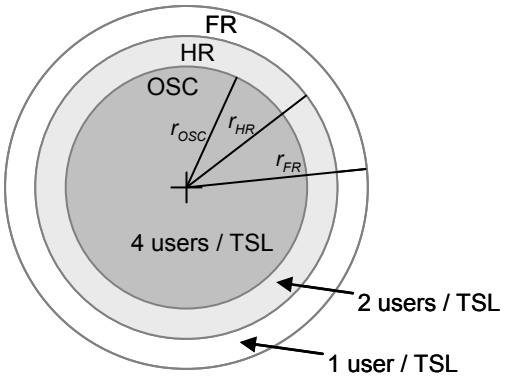

FIGURE 20. When OSC feature is activated, there will be functional areas for OSC DHR, HR and FR in the cell, each providing different capacity performance.

Step 4: Capacity estimate for the OSC and HR regions, and estimate of each region proportions. The division can be estimated by the HR and FR codec utilization statistics of BSC, U_{HR} indicating the utilization for HR (%) and U_{FR} indicating the utilization for FR (%). This division gives the first type of indicator for the capacity gain.

C. OSC utilization

During the laboratory measurements described above, the codec utilization measurement was not yet activated. In practice, the voice codec statistics measurement can be activated in BSC in the same manner as (Q, P_{RX}) statistics in order to obtain the realistic division of the HR and FR utilization. In this analysis, we can assume case values of U_{FR} = 10% and U_{HR} = 90%. The comparison is done by calculating first the reference situation, i.e., the total capacity utilization via HR and FR, by giving a weight of δ_{HR} = 2 (users / TSL) for HR (δ_{HR}) and 1 (users / TSL) for the FR (δ_{FR}):

$$U_{GSM}^{tot} = \delta_{FR} \cdot U_{FR} + \delta_{HR} \cdot U_{HR} = 1 \cdot 10\% + 2 \cdot 90\% = 180\% \quad (30)$$

The reference value is for full FR utilization, which results 100%. The HR mode as such gives thus 80% capacity gain in this specific example. When OSC is activated, the utilization of OSC and HR can be estimated accordingly, and the new capacity utilization can be thus calculated by:

$$U_{OSC}^{tot} = \delta_{FR} \cdot U_{FR} + \delta_{HR} \cdot U_{HR} + \delta_{OSC} \cdot U_{OSC} \quad , \quad (31)$$

where the weight for OSC users (δ_{OSC}) is 4 (users / TSL). Assuming the utilization is still 10% for FR, we get the new division between the HR and OSC utilization by observing the Q_4 criterion and CDF as shown in FIGURE 16. The respective division between the HR and OSC regions can be thus solved.

In this specific case of the laboratory results, by observing the FIGURE 16 and respective result via (30) and (31), the OSC utilization is 100–10.6 = 89.4 (%) compared to the original HR area. The remaining 10.6 (%) share of the area represents thus the new HR region. The total utilization of the capacity when OSC is activated is thus:

$$U_{OSC}^{tot} = 1 \cdot 10\% + 2 \cdot 10.6\% + 4 \cdot 79.4\% = 348.8\% \quad (32)$$

The original situation without OSC presenting a 100 % reference, this means that the capacity gain of Dual Half Rate OSC is 248.8% compared to the presence of only FR mode, and 348.8·100/180–100 = 93.8% compared to the presence of both, FR and HR modes.

It is possible to investigate further the dependency of the number of users and Erlang B formula's offered traffic as a function of the OSC penetration as shown in FIGURE 7, which shows the principle of the method with an example of 2% blocking rate. Other blocking rates are possible to be used as a basis for the calculations based on the statistics collected from the network. In order to estimate the capacity gain correctly, the investigation of the blocking rate of the network area of interest during the busy hour is thus needed.

FIGURE 7 summarizes the behavior of the channel utilization. It can be seen that the performance of the cell increases due to the Erlang B gain, along with the OSC penetration growth compared to the original proportion of the HR capable users.

D. TRX reduction gain

The calculation for the reduced GSM resources can be made by assuming that the offered traffic level and the call blocking rate are maintained in the original level. FIGURE 8 summarizes the analysis carried out for 20...100 Erl of offered traffic when the blocking rate is 2%.

As can be seen from FIGURE 8, along the growth of the OSC penetration, the needed number of TSLs with the same blocking rate (originally 2%) gets lower. According to the behavior of the Erlang B model, the effect is logically strongest for the higher capacity cells. This can be noted especially from the highest investigated offered traffic class of 100 Erl, which requires only half of the timeslots when OSC penetration is 100%.

Two cases can be constructed based on the offered traffic behavior of GSM as a function of OSC penetration. As a first case, the offered capacity can be maintained the same, which means that the blocking rate for the users will be lower (gain of lower blocking rate). This case applies also to the situation where future TRX expansions are planned they can be postponed until the original (or separately decided new) blocking rate is achieved.

If, instead, the offered capacity is lowered by keeping the blocking rate the same, we can estimate the OSC capacity gain in terms of the savings in the TRXs. This TRX reduction can be made based on TABLE 6, by taking into account that each TRX element should be informed as integer num-

ber that is rounded up (containing always 8 physical TSLs). Again, the blocking rate of 2% (or lower) is utilized as the criterion. The possibility to reduce the TRX elements can be utilized for the additional capacity for 3G and 4G.

TABLE 6. The estimation of the number of TRX elements that can be removed as a function of OSC penetration, when the blocking probability B=2%.

$\bar{x}$ (Erl)	OSC penetration				
	0.00	0.25	0.50	0.75	1.00
20	-	-	-	-	1
40	-	1	1	2	2
60	-	1	1	2	2
80	-	1	1	2	3
100	-	1	2	3	4

TABLE 6 indicates the capacity gain obtained as a function of the OSC penetration in terms of the TRX element reduction within the functional area of OSC. This case applies to the re-farming of the 2G, 3G and 4G frequencies.

The reduced need for the GSM bandwidth in order to still deliver the original 2G traffic with an unchanged quality of service level may provide the possibility to add a new UMTS carrier of 5 MHz [17] to the same band. As an example, if the original GSM band is of 10 MHz (50 channels of 200 kHz each), according to FIGURE 9, the 80 Erl traffic can be offered with half of the original amount of TRXs when the SAIC handset penetration is near 100%. This means that the original GSM traffic could be possible to deliver within 5 MHz band still maintaining approximately the same blocking rate, which leaves sufficiently space for adding a complete UMTS carrier as a parallel solution.

The benefit can also be seen with LTE, which provides more freedom to select the bandwidth, compared to the fixed 5 MHz band of UMTS. The narrowest LTE bands, i.e., 1.4, 3 and 5 MHz [18] can be utilized to the gradual increasing of LTE, when first, GSM traffic can be offered in smaller band by OSC, and when GSM traffic eventually lowers.

By applying the model and reference measurements for the quality effect of OSC in noise-limited environment, the optimal site configurations can be achieved. According to the results presented in this paper, the sites that contain at least 4 TRXs with approximately 2% blocking rate during the peak-hour, can benefit from the activation of OSC in such a scale that the 4-TRX cell with OSC penetration of about 25% would give possibility to remove one complete TRX, the blocking rate still being at the same or lower 2% level. Alternatively, if the SAIC penetration is relatively high, in order of 75%, one TRX element can be removed even from a 3-TRX cell without impacts on the blocking.

In the live network, the final effects of OSC depend on the proportion of the overlapping cells, co-channel interference levels, inter-cell handover algorithms and their parameter values. In any case, the presented analysis gives indication about the behavior of OSC when the OSC-paired HR calls, which can fit a maximum of four users to a single TSL, are switched back to HR mode that allows two users to a single TSL, or to FR mode that occupies the whole TSL for a single connection. The presented model shows how to estimate the proportion of these regions, and what the effect of OSC is on the final capacity compared to the network that supports only the basic mode of FR/HR.

VI. CONCLUSIONS

This paper shows the behavior of the OSC capacity and radio performance as a function of the OSC penetration by comparing it with the GSM HR/FR traffic. The presented analysis is based on theoretical studies of the capacity and traffic behavior, as well as on single cell indoor measurements in the non-interfering environment.

According to the analysis presented in this paper, the OSC might function in about 10% smaller coverage area than HR mode in a tightly dimensioned environment. This proportion depends on the network dimensioning, which should be taken into account in the interpretation of the presented results.

The results presented in this paper show that the OSC offers a SAIC capable MS penetration dependent capacity gain, which can be utilized for lowering the blocking rate of the GSM network. In this scenario, the OSC does not benefit only the voice capacity, but it also provides higher efficiency for the data calls as OSC leaves more time slots for the use of packet switched domain. As in this case, the OSC allows the circuit switched calls to be delivered via lower amount of TSLs, it also liberates TSLs for the PS calls resulting higher average data throughputs per data user. It also means that recently standardized DLDC (Downlink Dual Carrier) of GSM benefits from OSC as the probability to obtain TSLs from two separate carriers for DLDC users increases.

Alternatively, the OSC feature can be utilized for releasing a part of the TRXs still maintaining the same or lower blocking rate that is dimensioned for the GSM HR network. This scenario can be utilized for the frequency re-farming. Assuming that the renewal period of current GSM handsets is typically from 3 to 4 years, i.e., the OSC capable MS penetration grows relatively fast, the OSC functionality provides efficient parallel utilization of GSM and 3G/4G.

The presented method is based on the correlated received power level and quality measurements of BSC. It is shown that the matrix format, even if the utilized P_{RX} category ranges are relatively wide (from 5 to 10 dB resolution) due to the limitations of the statistics collection tool, can be utilized in the estimation of the OSC performance based on the quality measurements of the GSM network before the OSC is activated. The benefit of this method is that the statistics can be collected by activating the correlating data collection under the whole BSC area. The collected data is thus statistically considerably more accurate compared to a single mobile radio interface measurement results.

The results indicate the OSC performance in indoor radio channel that contains a relatively small proportion of fast fading components. The speed represents a typical slow-moving pedestrian type, and the cell is noise limited. The GSM HR codec was utilized for the reference. In case of other references (GSM FR and different AMR levels), and other radio conditions, additional measurements are needed for creating the M'_{diff} matrix, which would be a future work

item. Assuming the effect of the environment is low on the M'_{diff}, the results presented in this paper may be used as a general estimate of the OSC. As a future work item, the model will be evaluated in the outdoor environment with interfering components present.

The model can be considered useful because only basic KPIs and statistics about the OSC capable handset penetration is required as input values. The result of the model indicates the effect of the OSC for the combination of the radio performance and capacity behavior.

ACKNOWLEDGMENT

This work is based on the analysis and laboratory tests carried out at Nokia Siemens Networks Innovation Center (NICE), Madrid, Spain and collaborated with Vodafone. The laboratory setup by Mr. Mikko Nurkka and comments given by Mr. Luis Maestro and Mr. Kari Niemelä are gratefully acknowledged.

REFERENCES

[1] J. Penttinen, F. Calabrese, K. Niemelä, D. Valerdi, and M. Molina. Performance Model for Orthogonal Sub Channel in Noise-limited Environment. Conference proceedings. International Academy, Research, and Industry Association (IARIA). The Sixth International Conference on Wireless and Mobile Communications, ICWMC 2010. September 20-25, 2010, Valencia, Spain. 6 p.

[2] J. Penttinen, F. Calabrese, L. Maestro, K. Niemelä, D. Valerdi, and M. Molina. Capacity Gain Estimation for Orthogonal Sub Channel. Conference proceedings. International Academy, Research, and Industry Association (IARIA). The Sixth International Conference on Wireless and Mobile Communications, ICWMC 2010. Valencia, Spain, September 20-25, 2010. 6 p.

[3] Jose Gimenez, Pablo Tapia, Matti Salmenkaita, and Mariano Fernandez-Navarro. Analysis of dynamic frequency and channel assignment in irregular network environment. The 5th International Symposium on Wireless Personal Multimedia Communications. Volume 2, 2002, Pp. 863-867.

[4] Mikko Säily, Guillaume Sébire, and Eddie Riddington. GSM/EDGE: Evolution and performance. ISBN 978-0-470-74685-1. Wiley, Oct. 2010. 504 p.

[5] A. N. Barreto and R. Pirhonen. Capacity Increase in GSM Networks Using Source-Adaptive AMR. Vehicular Technology Conference, 2006. VTC 2006-Spring. IEEE 63rd, Volume 2. Pp. 553-557.

[6] M. H. Ahmed, W. Wei, and S. A. Mahmoud. Downlink Capacity Enhancement in GSM Systems with Frequency Hopping and Multiple Beam Smart Antennas. IEEE International Conference on Communications (ICC 2000), 18-22 June, 2000. Volume 2. Pp. 1015-1019.

[7] R. Meyer, W. H. Gerstacker, R. Schober, and J. B. Huber. A Single Antenna Interference Cancellation for Increased GSM Capacity. IEEE Transactions on Wireless Communications, Vol. 5, Issue 7. July 2006. Pp. 1616-1621.

[8] A. Mostafa, R. Kobylinski, I. Konstanic, and M. Austin. Single Antenna Interference Cancellation (SAIC) for GSM Networks. IEEE 58th Vehicular Technology Conference, 2003. VTC 2003-Fall. Pp. 1089-1093.

[9] X. Chen, Z. Fei, J. Kuang, L. Liu, and G. Yang. A Scheme of multi-user reusing one slot on enhancing capacity of GSM/EDGE networks. 11th IEEE Singapore International Conference on Communications Systems, November 2008. Pp. 1574-1578.

[10] M. Moisio and S. Nikkarinen. Capacity Gains of Single Antenna Interference Cancellation in GSM. Symposium on 15th IEEE International Personal, Indoor and Mobile Radio Communications (PIMRC) 2004. Volume 4, 2004. Pp. 2700-2704.

[11] Meeting report GP-081309. New WID on Voice services over Adaptive Multiuser Orthogonal Subchannels (VAMOS). 3GPP GERAN #39.

[12] 3GPP TR 45.903. Feasibility study on Single Antenna Interference Cancellation (SAIC) for GSM networks, V 8.0.0. 18 December 2008.

[13] Meeting report GP-071792. Voice Capacity Evolution with Orthogonal Sub Channels. Nokia Siemens Networks, 3GPP GERAN #36. November 2007.

[14] Technical Specification Group GERAN. Meeting Report. Meeting #42, Shenzhen, P. R. of China, 11 - 15 May, 2009. 229 p.

[15] 3GPP TS 05.05 V8.20.0 (2005-11). Technical Specification Group GSM/EDGE. November 2005. 100 p.

[16] S. Qiao. A Robust and Efficient Algorithm for Evaluating Erlang B Formula. Dept. of Comuting and Software, McMaster University, Canada. October 17, 1998. 8 p.

[17] Harri Holma and Antti Toskala. WCDMA for UMTS; HSPA evolution and LTE. ISBN 978-0-470-31933-8. Wiley, 2008. 539 p.

[18] Harri Holma and Antti Toskala. LTE for UMTS; OFDMA and SC-FDMA based radio access. ISBN 978-0-470-99401-6. Wiley, 2009. 433 p.

BIOGRAPHIES

Mr. Jyrki T.J. Penttinen has worked in telecommunications industry since 1994, for Telecom Finland and it's successors until 2004, and after that, for Nokia and Nokia Siemens Networks. He has hold mobile networks research, design and technical management positions in Finland, Spain, Mexico and USA. His special interests areas are related to the radio interface of GSM/3G evolution, LTE and mobile TV. He currently works in Senior Solutions Architect position with NSN Innovation Center, Madrid, Spain. Mr. Penttinen obtained his M.Sc., Lic.Sc. and D.Sc. degrees from Helsinki University of Technology (currently known as Aalto University, School of Science and Technology), Finland, 1994, 1999, and 2011, respectively.

Mr. Francesco D. Calabrese Graduated with a degree in Mobile Communications in September 2005 from Aalborg University (Denmark) and in Telecommunication Engineering in October 2005 from L'Aquila University (Italy). From September 2005 to September 2006 he worked as a researcher at the Department of Electronic Systems at Aalborg University collaborating with Nokia Siemens Networks on the design of Radio Resource Management algorithms for LTE. From September 2006 on he continued his research in the same area while pursuing a PhD degree, which he completed in June 2009. He has been with the Nokia Siemens Networks Innovation Center in Madrid (Spain) since July 2009, and is currently in charge of WCDMA and HSPA+ investigations.

Mr. David Valerdi holds a technical product manager position at Vodafone Group PLC, one of the largest mobile telecommunications network company in the world. With an extensive international experience in telecom sector, he was previously senior system engineer working for Telefonica and Motorola. David obtained telecoms engineering qualifications and became MBA graduated with honors in 2009, at Instituto de Empresa.

Mr. Iñigo Güemes has worked in mobile industry since 1998, for Airtel Móvil, its successor Vodafone Spain and Vodafone Group PLC. He has hold mobile networks design, optimization, technical management and business integration analyst positions in Spain and Germany. He currently works in technical Product Manager position at Vodafone Group PLC in Madrid (Spain). Mr. Güemes graduated with a degree in Radio Telecommunication Engineering in November 1998 from Basque Country University (UPV /EHU, Spain) and became MBA in 2009, at Escuela de Organización Industrial (EOI, Spain).